Spodoptera frugiperda transcriptional response to infestation by *Steinernema carpocapsae*

Fall Armyworm transcriptional response to nematode infestation

Louise Huot[1], Simon George[1], Pierre-Alain Girard[1], Dany Severac[2], Nicolas Nègre[1,*] and Bernard Duvic[1,*]

[1] DGIMI, Univ Montpellier, INRA, Montpellier, France

[2] MGX, Univ Montpellier, CNRS, INSERM, Montpellier, France

[*] Co-corresponding authors

E-mail: nicolas.negre@umontpellier.fr (NN) ; bernard.duvic@umontpellier.fr (BD)

Abstract

Steinernema carpocapsae is an entomopathogenic nematode (EPN) used in biological control of agricultural pest insects. It enters the hemocoel of its host via the intestinal tract and releases its symbiotic bacterium *Xenorhabdus nematophila*, which kills the insect in less than 48 hours. Although several aspects of its interactions with insects have been extensively studied, still little is known about the immune and physiological responses of its different hosts. In order to improve this knowledge, we examined the transcriptional responses to EPN infestation of the fat body, the hemocytes and the midgut in the lepidopteran pest model *Spodoptera frugiperda* (Lepidoptera: Noctuidae).

Our results indicate that the tissues poorly respond to the infestation at an early time post-infestation of 8 h, even though the proliferation of the bacterial symbiont within the hemocoel is detected. Only 5 genes are differentially expressed in the fat body of the caterpillars. However, strong transcriptional responses are observed at a later time point of 15 h post-infestation in all three tissues. While few genes are differentially expressed in the midgut, tissue-specific panels of induced metalloprotease inhibitors, immune receptors and antimicrobial peptides together with several uncharacterized genes are up-regulated in the fat body and the hemocytes. In addition, among the most up-regulated genes, we identified new potential immune effectors, unique to Lepidoptera, for which we present evidence of acquisition by Horizontal Gene Transfer from bacteria.

Altogether, these results pave the way for further functional studies of the mobilized genes' involvement in the interaction with the EPN.

Author summary

The Fall Armyworm, *Spodoptera frugiperda*, is a major agricultural pest. The caterpillars cause extensive damage to crops of importance such as corn, rice, sorghum and cotton. Originally from the Americas, it is currently becoming invasive in other parts of the world, first in Africa in 2016, then in India and now in south-east Asia. Programs of biological control against insect pests are increasingly encouraged around the world and include the use of pathogens. Entomopathogenic nematodes such as *Steinernema carpocapsae* are already commercialized as organic pesticides. These nematodes live in the soil and enter the body of their insect preys. Once within the insects, they release their symbiotic bacteria (*Xenorhabdus nematophila* in this case), which infect and kill the host in a few hours. The nematodes can then feed on the dead insects, reproduce and resume their life cycle. It is a major challenge to understand how EPN achieve their pathogenicity as well as how the insects can resist them. Here we provide the foundation for such an interaction between EPN and a Lepidoptera. We analyzed the dynamic of transcriptional response in three insect tissues (midgut, fat body and hemocytes) upon infestation by EPN. Not many studies have been performed genome-wide on such an interaction, and none on a Lepidopteran model of economical importance. Our transcriptomic approach revealed some specificities of the Lepidopteran defense mechanisms. In particular, we discovered a set of genes, acquired in Lepidoptera from bacteria by Horizontal Gene Transfer, that probably encode proteins with antibiotic activity.

Introduction

There is a growing desire in Europe to reduce the use of chemical pesticides on agricultural land, because of their toxicity for the environment and human health (European Directive EC91/414). Also, the development of alternative methods for the control of crop pests is encouraged. These methods include the use of predators and pathogens of insect pests such as viruses, bacteria, fungi, parasitoid wasps and entomopathogenic nematodes (EPN).

EPN of the genus *Steinernema* associated with the symbiotic bacterium *Xenorhabdus* are among the most widely used and studied biological control agents (1). They pose little threat to human health and non-target species (2), but are capable of killing a broad spectrum of insect pests including the moth *Spodoptera frugiperda* (Lepidoptera: Noctuidae)(3, 4). The infestation cycle of the nematode *Steinernema carpocapsae* has been well described. It starts with the entry of infective juvenile larvae (IJ) into the insect intestinal tract via the natural orifices (5). Once the intestinal epithelium is crossed, EPN are found in the hemocoel where they release their symbiotic bacteria *Xenorhabdus nematophila*. The latter cause the death of the insect by toxemia and sepsis in less than 48 h. EPN multiply by feeding on the insect tissues, reassociate with their symbiotic bacteria (6) and then go back to the environment in search for a new prey (7).

Insects live in environments contaminated by microorganisms (bacteria, fungi or viruses) potentially pathogenic for them. To defend themselves against these aggressors, insects have developed a powerful and diversified immune system essentially based on innate immunity and which has been well described in the *Drosophila* model (8). Its main mechanisms and pathways seem to be conserved in different orders of insects (9-11) even though some insects, such as *Apis mellifera* or *Acyrthosiphon pisum*, have reduced immune repertoire (12, 13). The first line of defense are physical barriers, including the cuticle, which covers almost all insects' interfaces with the environment, and the peritrophic matrix, which replaces the cuticle in the

78 midgut (14). The cuticle is a thick exoskeleton made of wax, chitin and sclerotized proteins
79 that confers mechanical protection against wounds and invaders (15), while the midgut
80 peritrophic matrix is a thinner network of chitin and proteins that allows the uptake of nutrients
81 but which has a low permeability to microorganisms and toxins (16). The intestinal epithelium
82 can produce several immune molecules such as antimicrobial peptides (AMP) or reactive
83 oxygen species depending on the location (14). Once into the hemolymph, parasites are facing
84 circulating hemocytes, which are the immune blood cells of insects. Hemocytes participate in
85 sclerotization, coagulation as well as in the elimination of small pathogens (bacteria and yeasts)
86 by phagocytosis and nodulation, and of large pathogens (parasitoid wasp eggs, nematodes) by
87 encapsulation (17). Encapsulation, nodulation and coagulation may involve a process of
88 melanisation, which results in the formation of melanin and toxic chemicals that help to
89 sequester and to kill the pathogen (18). Melanisation is activated by an extracellular proteolytic
90 cascade, the pro-phenoloxidase system, following the recognition of microbial determinants or
91 danger signals (19). Finally, the systemic response of insects relies mainly on the massive
92 secretion of AMP by the fat body into the hemolymph, after activation of the IMD and/or Toll
93 pathways. The IMD pathway is primarily activated by peptidoglycan recognition proteins
94 (PGRP) in response to Gram-negative bacteria and the Toll pathway by PGRP and Gram
95 negative binding proteins (GNBP) in response to Gram-positive bacteria and fungi (20). The
96 Toll pathway may also be activated by exogenous proteases from pathogens (21).
97 Recently, different studies performed in the model insect, *Drosophila melanogaster*, described
98 the responses of this insect to two EPN, *Steinernema carpocapsae* or *Heterorhabditis*
99 *bacteriophora* (22-24). By the use of transcriptomic approaches on whole larvae or adult flies,
100 the authors showed the overexpression of a large number of immune-related genes involved in
101 defense responses such as coagulation, melanisation and the production of antimicrobial
102 peptides, and in several immune and stress-reponse pathways (Toll, Imd, Jak/Stat or JNK).

In this study, we carried out a transcriptomic analysis of physiological and immune responses of 6th instar larvae of *S. frugiperda* fat body, hemocytes and midgut at two time points after infection with the EPN *S. carpocapsae*. At 8 hours after infestation (hpi), we found only 5 genes that were differentially expressed in the fat body. However, at 15 hpi, we detected the significant expression modulation of 271 genes. Few genes were differentially expressed in the midgut whereas strong transcriptional responses were observed in the fat body and the hemocytes. These responses consisted mainly in the overexpression of induced metalloprotease inhibitors (IMPI), immune receptors (mostly PGRP) and AMP, indicating that the fat body as well as the hemocytes produce potent immune responses. Among the most up-regulated genes, we identified a cluster of new potential immune effectors, unique to Lepidoptera, for which we present evidence of acquisition by Horizontal Gene Transfer from bacteria. Finally, we identified a cluster of genes that are overexpressed in all tissues, but whose function is unknown and which are restricted to some noctuid species.

Results and discussion

EPN infestation and pathogenicity

To measure how *S. frugiperda* larvae respond to entomopathogenic nematodes (EPN), we performed infestation experiments where 6th instar larvae were individually put in contact with either Ringer solution (control experiment) or a solution of EPN in Ringer (infestation condition) at time T = 0 (see Methods and **Fig 1A**). We targeted two time points after infestation based on our previous knowledge of the mode of infestation (6). Eight hours post infestation (hpi), nematodes are supposed to have travelled in the intestinal tract of *S. frugiperda* larvae, crossed the intestinal barrier and started releasing their symbiotic bacteria, *Xenorhabdus nematophila*, within the hemocoel of the caterpillar (6). At 15 hpi, bacteria have multiplied and septicemia is supposed to be reached. In order to verify these assertions, we quantified the *X. nematophila* cells into the hemolymph by CFU counting on a selective medium. In parallel, the survival of the caterpillar to the EPN infestation was monitored for 72 h. Our data show that bacterial growth has already started at 8 hpi, from few bacterial cells released to 10^4 cells/mL of hemolymph and up to 10^6 cells/mL at 15 hpi, which is considered septicemia (**Fig 1B**). When we measured survival of the larvae following infestation, we observed that the first deaths occur at 28 hpi. At 72 hpi, almost all treated larvae were dead (**Fig 1C**) whereas no death was observed in the control experiments.

At 8 hpi and 15 hpi, we removed the larvae from either the control or the infestation plates and dissected three tissues: the midgut (MG), the fat body (FB) and the hemocytes (HC at 15 hpi only). From these tissues, RNA was extracted and processed to perform single end 50 bp Illumina sequencing on three biological replicates (**Fig 1A**). We recovered between 10 and 100 million reads per sample, of which between 50 and 70% align onto the reference transcriptome for *S. frugiperda* (25) (see Methods and **Table 1**). After normalization with DESeq2 (26), we

140 observed that gene expression datasets cluster by tissue (**S1 Fig**) and that within tissues,
141 condition replicates correlate well with each other.

142 **Table 1**: RNAseq statistics

Tissue	Condition	Sample	Total reads	Mapped reads	% Mapped reads
Fat body	Control 8 h	3FBn8	29 360 077	16 556 358	56.4
		5FBn8	28 766 960	16 431 320	57.1
	Control 15 h	1FBn15	8 160 217	5 760 726	70.6
		3FBn15	31 182 081	21 405 010	68.7
		5FBn15	101 295 028	67 865 194	67.0
	Infected 8 h	3FBi8	18 680 946	10 924 308	58.5
		5FBi8	27 084 597	13 484 897	49.8
	Infected 15 h	1FBi15	38 001 141	22 705 073	59.8
		3FBi15	25 680 693	15 233 458	59.3
		5FBi15	17 018 902	9 757 977	57.3
Midgut	Control 8 h	1MGn8	40 762 942	26 432 615	64.8
		3MGn8	37 701 095	24 444 804	64.8
		5MGn8	39 108 039	23 913 146	61.2
	Control 15 h	1MGn15	53 104 319	33 125 675	62.4
		5MGn15	56 673 439	35 116 354	62.0
	Infected 8 h	1MGi8	39 503 925	25 273 765	64.0
		3 MGi8	45 389 710	29 365 492	64.7
		5MGi8	33 930 844	21 504 374	63.4
	Infected 15 h	1MGi15	46 822 381	28 888 031	61.7
		3MGi15	40 929 947	25 691 178	62.8
		5MGi15	42 270 370	26 081 101	61.7
Hemocytes	Control 15 h	1HCn15	36 819 698	20 610 325	56.0
		3HCn15	41 399 767	23 008 997	55.6
		5HCn15	30 657 274	17 119 548	55.8
	Infected 15 h	1HCi15	32 486 507	18 101 920	55.7
		3HCi15	73 456 056	40 045 769	54.5
		5HCi15	33 712 769	18 309 356	54.3

143 *Samples abbreviations*: MG, midgut ; FB, fat body ; HC, hemocytes ; n, naive larvae ; i, infected larvae
144 ; Number at the end (8 or 15) corresponds to the time of tissue extraction after infestation with
145 nematodes.
146

147 ## Overview of transcriptional response

148 In MG and FB, at 8 hpi, we detected a very small transcriptional response with only 5

149 statistically significant differentially expressed (DE) genes in FB and none in MG (**S2 Fig**).
150 From these, 4 genes are overexpressed in response to infestation and are also retrieved
151 overexpressed at later time-points in all 3 tissues (**S3 Fig**). They are annotated in the genome
152 as unknown transcripts.
153 At 15 hpi, there is a more important transcriptional response with thousands of DE genes in all
154 three tissues at padj < 0.01 (**S2 Fig**), with in each case, more genes overexpressed than
155 underexpressed. In order to detect the most significant genes responding to EPN infestation at
156 15 h, we modeled the EPN effect across all datasets and identified 271 DE genes (**Fig 1D**)
157 which we intersected with all previous 1 on 1 comparison per conditions (see **Methods**). Of
158 these, we identified a total of 216 DE genes at 15 hpi in the three different tissues (**Fig 1E**).
159 Most of the response occurred in FB and HC tissues (**Fig 1E, Table 2**) with, again, a vast
160 majority of overexpressed genes (**Fig 1D** and **1E, Table 2**).
161 The data obtained by RNAseq were confirmed by quantitative RT-PCR on a selection of DE
162 genes in the three tissues (**S4 Fig**).

163 **Table 2**: Differentially expressed genes per condition at 15 hpi

Tissue	Midgut (MG)	Fat body (FB)	Hemocytes (HC)
Differentially expressed genes (padj<0.01)	54	125	189
Overexpressed genes (padj<0.01, Log2FC>0)	41 (75.9 %)	115 (92.0 %)	182 (96.3 %)
Underexpressed genes (padj<0.01, Log2FC<0)	13 (24.1 %)	10 (8.0 %)	7 (3.7 %)

164

165 Functional response of the Midgut at 15 hpi

166 The first line of defense against *S. carpocapsae* EPN is the midgut barrier, which is also the
167 main entry point of *Steinernema* nematodes in *S. frugiperda*. This organ is known for its
168 immune activity through the production of reactive oxygen species and anti-microbial peptides

169 in response to pathogens (27). It is not supposed to be directly confronted to *X. nematophila*
170 and therefore, we hypothesized that the genes, which would be overexpressed specifically in
171 the midgut may identify anti-nematode factors. However, we did not find any DE genes in the
172 midgut at 8 hpi and only 4 genes that were DE specifically in the midgut tissue at 15 hpi, with
173 only 1 being overexpressed and 3 under-expressed (**Fig 2A**). The overexpressed gene encodes
174 a heat-shock protein of the hsp70 family (**S1 Data**). This superfamily of genes is usually
175 upregulated in response to oxidative stress and in the midgut of *Drosophila*, Hsp68 promotes
176 the proliferation of intestinal stem cells, and thus its regeneration (28).
177 One of the under-expressed genes is an E3 ubiquitin-protein ligase of the Seven In Absentia
178 family (SIAH). The mammalian homologue Siah1 cooperates with SIP (Siah-interacting
179 protein), the F-box protein Ebi and the adaptor protein Skp1, to target beta-catenin, a
180 multifunctional protein that plays an important role in the transduction of Wnt signals and in
181 the intercellular adhesion by linking the cytoplasmic domain of cadherin, for ubiquitination
182 and degradation via a p53-dependent mechanism. Thus, down-regulation of SIAH might
183 increase levels of ß-catenin, which favors proliferation of intestinal stem cells in *Drosophila*
184 (14).
185 The two other under-expressed genes are an ABC family transporter and an NT-C2 domain
186 protein, for which no obvious link to infection or to intestinal homeostasis can be established
187 from the literature.
188 While we found no evidence of a direct response to EPN specifically by the midgut, we
189 investigated whether this tissue may share a common immune response with the fat body or
190 the hemocytes.
191 We found nine common DE genes between the midgut and the fat body, which are all
192 overexpressed in both tissues (**Fig 2B**). Of those, three genes have no annotated structure or
193 function. Four other genes with no clear homology have domains that can be associated to

194 regulation (protein-kinase domain, calcium binding domain, amino-acid transporter and
195 MADF domain transcription factor) (**S1 Data**). Interestingly, we found a cytochrome P450
196 gene encoding the CYP340L16. CYP genes are usually involved in detoxification of foreign
197 chemicals such as plant xenobiotics and pesticides (29). Finally, one trypsin inhibitor-like
198 cysteine rich domain proteinase inhibitor was also overexpressed. There is no enrichment for
199 a specific molecular function or biological process among those nine genes.
200 Similarly, 10 genes were found significantly differentially expressed in both the midgut and
201 hemocytes, with 6 of them being overexpressed in both tissues and 4 being under-expressed in
202 MG and upregulated in HC (**Fig 2C**). Of the 6 overexpressed genes, 4 are small solute
203 transporters of the Major Facilitator Superfamily (MFS), 1 is an antennal carboxylesterase and
204 1 is a proteinase inhibitor (**S1 Data**). No particular function of note has been identified for the
205 4 genes that were under-expressed in MG but overexpressed in HC, except for Iap2, which is
206 an inhibitor of apoptosis and a member of the IMD pathway (30).
207 From this comparison, it seems likely that the midgut is not specifically mobilized to defend
208 the *S. frugiperda* larvae against EPN infestation. There are few DE genes in this tissue, whether
209 specific or in common with other tissues, and no specific functional pathway can be clearly
210 identified. Rather, some of the genes identified may be reacting to oxidative stress and
211 homeostasis maintenance of the intestinal epithelium, which might be consequences of the host
212 infestation.

213 **Specific response of the fat body at 15 hpi**

214 In insects, the adipocytes that compose the fat body are in direct contact with the hemolymph.
215 The physiological function of this organ is to store energetic reserves, in the form of glycogen
216 and lipids, and release them if needed (31). It is also the main tissue involved in systemic
217 immunity, since it produces AMP during immune challenge (8). We found 14 DE genes

specifically in the fat body, with 12 overexpressed and 2 under-expressed genes. Among the latest are 1 uncharacterized protein and 1 putative transposable element (TE). Among the 12 fat body-specific up-regulated genes, we found one major actor of immunity, the Toll receptor (32), which recognizes the cleaved circulating cytokine Spätzle to induce the production of anti-microbial peptides (33). It is noteworthy that Toll receptor is expressed in all three tissues, but overexpressed in response to EPN in the fat body only (**Fig 3A**). Among the 11 other overexpressed genes, we found one potential receptor of the arrestin family, several enzymes (lipase, carboxypeptidase and a GTPase co-factor), again a MADF-domain transcription factor and a dynein (**S1 Data**).

Specific response of the hemocytes at 15 hpi

In insects, hemocytes are the main actors of the cellular immune responses like phagocytosis or encapsulation (34). They are also involved in other defense mechanisms such as coagulation (35), and melanization (36, 37). In addition, different reports have shown that hemocytes are, as the fat body, capable of synthesis of AMP (38-40). Therefore, we hypothesized that genes specifically induced in the hemocytes may be involved in coagulation and/or melanization along with cellular immune responses.

The largest number of DE genes is found specifically in the hemocytes with 77 genes (**Fig 1E**), of which 74 are overexpressed in response to EPN infestation (**Fig 3B**). No enriched GO categories have been detected in this list. However, we noticed several categories of genes of interest. The most overexpressed gene encodes a serine protease without CLIP-domain (**S1 Data**) that is homologous to hemolymph proteinase 7 (HP7) and 10 (HP10) in *Manduca sexta* (41). In the insect immune system, serine proteases participate in the activation of Toll-dependent response to infection as well as in the PPO-dependent melanization cascade (42). However, many serine-proteases, in particular without CLIP-domains such as HP7 & HP10,

still have unknown function. They are regulated by protease inhibitors, a large family of small peptides, one of which is also found highly induced in our list (**S1 Data**) (log2FoldChange = 8.06). This induction suggests a specific role of HP7/HP10 in the hemocytes activation after infestation by EPN.

The molecular functions we encountered in the hemocytes specific gene list include MFS transporters, ubiquitin-conjugating enzymes, sina-like, antennal esterases, heat-shock proteins and several protein kinases. We also noticed several genes that may play a role in vacuolar trafficking and signaling, with several transmembrane domain proteins. The general molecular function of these genes makes it hard to link them to any biological process.

Surprisingly, we noticed that very few genes linked to immunity were present in this list. In particular, we have not found a deregulation of genes linked to the activation of the PPO pathway besides the above-mentioned serine proteases. The only gene that we could relate to melanization is homologous to the L-dopachrome tautomerase Yellow-f2 that is responsible for the conversion of DOPA into dopamine, a precursor of melanin.

Three transcription factors are also found overexpressed in HC, including Vrille. Vrille is known to activate the serine protease Easter that, in turns, cleaves the Spätzle protein that is the ligand of Toll receptor, which we found overexpressed in the fat body (see above). Other genes involved in immunity are Pellino which might be either a negative regulator (43) or an enhancer (44) of the Toll pathway, and IMD which is a member of the IMD pathway.

Common response of the Fat Body and the Hemocytes at 15 hpi

We identified 71 genes differentially expressed upon EPN infestation in both FB and HC tissues (**Fig 1E**), 66 of them being overexpressed in both tissues. The "immunity" ontology is the most enriched GO category (**S5 Fig**). The most overexpressed genes correspond to a battery of anti-microbial peptides (attacins, cecropins, defensins, gloverins and moricins) (**S1 Data**).

We identified by homology a repertoire of 40 AMP in the genome of *S. frugiperda*, classified in 7 different families (25). The majority of AMP production is performed by the FB tissue with members of the attacins, cecropins, gloverins and lebocins strongly overexpressed (**Fig 3C**). These AMP are also significantly overexpressed in the HC but to a lesser extent (**Fig. 3C**). Defensins such as the gallerimycin (45) and Spod-x-tox (46) are overexpressed in both tissues. Remarkably, of the 10 moricins present in *S. frugiperda* genome, only Moricin 10 is strongly overexpressed in both tissues. The diapausin overexpression is less clear with low levels of expression.

Among the most overexpressed genes in both FB and HC tissues, we also identified several members of the peptidoglycan recognition proteins (PGRP) (**S1 Data**), a family of receptors, which are involved in the recognition of pathogens associated molecular patterns (PAMP) and in the subsequent activation of the Toll, Imd and PPO system pathways (19, 20). In the genome of *S. frugiperda*, we identified 10 PGRP (**S6A Fig**) that were named according to *Bombyx mori* nomenclature (9). Upon EPN infestation, PGRP-S2, -S6 and -L3 are overexpressed in both FB and HC, with PGRP-S2 being the highest overexpressed (**S1 Data**). A phylogenetic analysis (**S6B Fig)** shows that PGRP-S2 is closely related to *Drosophila melanogaster* PGRP-SA, which is involved in the induction of the Toll pathway (47). Recently, it has also been reported that a PGRP-SA homolog may be responsible for the activation of the phenoloxidase system in the Chinese tussar moth *Antheraea pernyi* (48).

This overexpression of AMP and PGRP upon EPN infestation has been similarly observed in transcriptomic studies of *Drosophila melanogaster* larvae infested by *Heterorhabditis* sp. or *Steinernema* sp. nematodes (22-24).

Other immunity genes overexpressed in both tissues are implicated in the Toll pathway. This pathway is activated by PAMP recognition proteins or by proteases from pathogens (21, 49). Signal is transduced by an intracellular complex (MyD88/Tube/Pelle) that binds to the

intracytoplasmic domain of Toll and is regulated by Pellino (43, 44). Signal transduction results in the phosphorylation of the ankyrin-repeat containing protein Cactus, which allows its dissociation from the transcription factor Dorsal. This dissociation promotes the translocation of Dorsal to the nucleus where it activates the production of AMP. Several members of this pathway are overexpressed in both FB and HC at 15 hpi, including Pelle, Pellino, and Cactus. Altogether, these results suggest that the Toll pathway is activated in both the fat body and the hemocytes.

We also observed the overexpression of Hdd23 which mediates PPO activation (50) and of 3 putative transcription factors, one of them containing a zinc-finger domain (GATA4-like) known to mediate immune response in *Drosophila* (51).

In addition to immune-related genes, this list contains 7 protease inhibitors. One is a serine protease inhibitor, which may be involved in the regulation of serine proteases cascades, such as the prophenoloxidase activating cascade (42) or the Toll activating cascade (8), while another has homology with a tissue inhibitor of metalloproteases (TIMP). More interestingly, the 5 remaining protease inhibitors belong to the family of inducible metalloprotease inhibitors also called IMPI (52). These 5 IMPI are present as a cluster of genes in the genome of *S. frugiperda* (**Fig 4A**) and their expression is upregulated especially in the hemocytes (**Fig 4B**). The first IMPI was purified from the hemolymph of the greater wax moth *Galleria mellonella* (53) and further cloned (54). The expression of IMPI, along with antimicrobial peptides/proteins, is induced by metalloproteases released by damage tissue or metalloproteases from pathogens during the humoral immune response of *G. mellonella* (52). It is well known that entomopathogenic bacteria, such as *X. nematophila* or *Bacillus thuringiensis*, establish their pathogenesis by secreting virulence factors among which metalloproteases (55-59). Therefore, we may hypothesize that *S. frugiperda* induces the expression of IMPI to counteract the metalloproteases produced by *X. nematophila*.

316 ## Common response of the Midgut, the Fat body and the Hemocytes at 15 hpi

317 Finally, we identified 31 genes that are significantly differentially expressed in all three tissues
318 (MG, FB and HC), 25 of them being overexpressed in all tissues (**Fig 1E, S1 Data**). There is
319 no enrichment for a specific molecular function or biological process among these 25 genes
320 and only 3 of them could be related to the caterpillar defenses. They encode the previously
321 cited Hdd23 and Cactus, plus Relish, the transcription factor of the Imd pathway, suggesting
322 that this anti-Gram negative bacteria immune pathway (60) could also take part in the
323 previously described humoral responses.
324 During the annotation of these genes, we noticed that the 4 most differentially expressed genes
325 had no known function. Three of them were also among the few that were overexpressed in the
326 FB at 8 hpi (**Fig 5A**). We pursued the investigation on the potential origin of these genes, which
327 led us to the identification of 2 previously uncharacterized clusters (**Fig 5B and 5C**).
328 The first cluster (**Fig 5B**) is composed of 5 genes for which we could not find any homology
329 in sequence databases at the protein nor at the nucleotide level in any other organism than
330 *Spodoptera frugiperda*. However, we could find the whole cluster in the Sf9 and Sf21 cell lines
331 genomes recently published by other labs (61, 62). In addition, after careful exploration of the
332 syntenic regions, this cluster was also identified in the genomes of two other noctuid species,
333 *Spodoptera litura* and *Helicoverpa armigera* (63, 64). Interestingly, the cluster is located close
334 to a gene homolog to the *D. melanogaster* tamozhennic, which has been reported to be involved
335 in Dorsal nuclear translocation (65). Their genomic localization, their organization in cluster,
336 the presence of eukaryotic signal peptides in their predicted amino acid sequences, the fact that
337 they were not only the most differentially expressed genes upon EPN infestation but also the
338 earliest differentially expressed, led us to the hypothesis that they might encode a new class of
339 immune effectors restricted to some noctuid species.

A second intriguing category of genes in this list has a homology to bacterial proteins of unknown function. They are a set of three genes in cluster (**Fig 5C**), localized between several defensin encoding genes. They possess a eukaryotic peptide signal and two introns but their main coding sequence is homologous to genes from the *Lactococcus lactis* bacteria (**S7 Fig**) and shares a homology with a cysteine peptidase domain of the papain family. Among insects, these genes are found only in the genomes of other Lepidoptera (**S7 Fig**). Acquisition of antimicrobial activity from bacteria to eukaryotes by horizontal gene transfer (HGT) has been documented before (66), but not in insects. The genes we discovered by transcriptomic here might represent a Lepidoptera specific expansion of immune competence by acquisition of bacterial genes.

Conclusions

In this work, we have conducted a time-series analysis of tissue-specific transcriptomic response of the Lepidoptera *Spodoptera frugiperda* larvae to the infestation by the EPN complex *Steinernema carpocapsae*/*Xenorhabdus nematophila*. We show that at 8 hours after infestation only a few genes are mobilized in the fat body and none in the midgut, despite the presence and amplification of the EPN symbiont *X. nematophila* in the hemocoel. However, we observed a strong response of the larvae at 15 hours post infestation. This response corresponds to a complementary activation of the immune system by the fat body and the hemocytes, resulting in the production of a large repertoire of humoral effectors and receptors. When we compare our data to RNAseq analyses performed by other laboratories, albeit on different interaction systems, we observe a very similar response. For example, Castillo et al. (2015) report an activation of the immune system of *Drosophila melanogaster* larvae by the EPN complex *Heterorhabditis bacteriophora*/*Photorhabdus luminescens*, represented by several AMPs, several peptidase and protease inhibitors and also Yellow-F. This suggests that all potential hosts possess a conserved ability to fight against EPN complexes.

Despite this powerful response, *S. carpocapsae*/*X. nematophila* complex will be successful regardless of the system they will be confronted with. Anatomies of their host might differ but IJs will find their way inside the midgut and pierce it to enter the hemocoel. There, they will survive the inflammatory response of their host for a sufficient amount of time in order for their released bacterial symbionts to multiply within the insect and kill it (6, 7, 67). It was proposed that the nematodes were able to camouflage themselves from the insect immune system (68). The facts that we found very few genes mobilized at the early time point of 8 hpi and that very few immune-related genes were found mobilized in the midgut at any time point support this idea. However, despite a previous study suggesting that *X. nematophila* could resist to the humoral immune responses by transcriptional down-regulation (69), our study and recent

376 others (24, 70) clearly show that, regardless of the host insect, the immune system is triggered
377 and will react to the EPN infestation.
378 Nothing in our data suggests a mechanism by which the EPNs bypass the insect defenses at 15
379 hpi. Indeed, at this time point, all signaling pathways seem activated in both the fat body and
380 the hemocytes and 16 different AMP are produced. Several studies have evidenced a loss of
381 hemolymph AMP and antimicrobial activity during infection by the EPN or by *X. nematophila*
382 (71, 72). A likely hypothesis might be that these AMP are degraded by *X. nematophila*
383 virulence factors, as shown for the *X. nematophila* protease II in *Galleria mellonella* and
384 *Pseudaletia unipuncta* (56).
385

Materials and Methods

Insect rearing

Corn variant *Spodoptera frugiperda* (Lepidoptera : Noctuidae) larvae were reared on a corn-based artificial diet (73). They were maintained at 23°C +/- 1°C with a photoperiod of 16 h/8 h (light/dark) and a relative humidity of 40% +/- 5%. *Galleria mellonella* (Lepidoptera : pyralidae) larvae were reared on honey and pollen at 28°C in dark.

Nematode production and storage

Symbiotic *Steinernema carpocapsae* (strain SK27 isolated from Plougastel, France) were renewed on White traps (74) after infestation of the wax moth *Galleria mellonella* last larval stages. They were maintained in aerated Ringer sterile solution with 0.1 % formaldehyde at 8°C for two to four weeks to ensure optimal pathogenicity.

Infestation

Infestation experiments were processed at 23°C in 12-well culture plates. In each well, one second day sixth instar larva of *S. frugiperda* was placed on a filter paper (Whatman) with artificial corn-based medium. For infested larvae, 150 µL of Ringer sterile solution containing 150 *S. carpocapsae* IJs were introduced in each well. 150 µL of Ringer sterile solution was used for control larvae. To control the nematodes' efficacy, the survival of 12 larvae in both conditions was monitored for 48 hours in each experiment.

Xenorhabdus nematophila quantification

The concentration of *X. nematophila* in *S. frugiperda* hemolymph after infestation was estimated by CFU counting on NBTA (nutrient agar supplemented with 25 mg of bromothymol blue per liter and 40 mg of triphenyltetrazolium chloride per liter) with 15 µg/mL of

erythromycin. For 3 independent experiments and 3 technical replicates, hemolymph was collected by bleeding of 3 caterpillars in 200 µL PBS buffer supplemented with phenylthiourea. The volumes of hemolymph were then estimated and serial dilutions of the samples were plated. CFU were counted after 48 h incubation at 28°C and CFU numbers were then reported to the estimated hemolymph volumes in order to calculate the bacterial concentrations. The hemolymph of naive caterpillars was also plated to verify the absence of bacterial growth.

RNA extraction

Spodoptera frugiperda larvae were bled and hemolymph was collected in anti-coagulant buffer (75). Hemocytes were recovered by a short centrifugation at 800 g for 1 min at 4°C. The hemocyte pellet was immediately flash-frozen. Then, larvae were dissected and fat bodies and midguts were extracted, rinsed with PBS, flash-frozen with liquid nitrogen in eppendorf tubes and conserved at -80°C until use. After thawing, 1 mL of Trizol (Life technologies) was added and pooled organs were grounded with a TissueLyzer 85210 Rotator (Qiagen) with one stainless steel bead (3 mm diameter) at 30 Hz for 3 min. Grounded tissues were transferred in new eppendorf tubes and left at room temperature for 5 min then 200 µL of chloroform (Interchim) were added. The preparations were homogenized and left at room temperature for 2 min. After a centrifugation at 15,000 g and 4°C for 15 min, the aqueous phase was transferred in new eppendorf tubes. Four hundred µL of 70% ethanol were added and nucleic acid extraction was immediately done with the RNeasy mini kit (Qiagen) according to the manufacturer's instructions. Contaminating DNA was removed by the use of a Turbo DNA-free™ kit (Life Technologies) according to the manufacturer's protocol.

RNA yield and preparation purity were analyzed with a Nanodrop 2000 spectrophotometer (Thermo Scientific) by the measure of the ratios A_{260}/A_{280} and A_{260}/A_{230}, respectively. RNA

integrity was verified by agarose gel electrophoresis. RNA preparations were then conserved at - 80°C.

Library preparation and Illumina sequencing

Library preparation and RNA sequencing were conducted by MGX GenomiX (IGF, Montpellier, France). Libraries were prepared with the TruSeq Stranded mRNA Sample preparation kit (Illumina). In brief, after a purification step with oligo(dT) magnetic beads, polyadenylated RNAs were chemically fragmented. A first cDNA strand was synthesized with random primers and SuperScript IV Reverse Transcriptase (Life Technologies) and the second strand was then synthesized. After the addition of single adenine nucleotides, indexed adapters were ligated to the cDNA ends. Adapters-ligated cDNAs were then amplified by PCR and libraries were validated on Fragment Analyzer with a Standard Sensitivity NGS kit (Advanced Analytical Technologies, Inc) and quantified by qPCR with a Light Cycler 480 thermal cycler (Roche Molecular diagnostics).

cDNAs were sequenced with the HiSeq 2500 system (Illumina) on 50 base pairs with a single-end protocol. In brief, libraries were equimolary pooled and cDNAs were denatured, diluted to 8 pM and injected in the flow cell. The samples were multiplexed by 6 and a PhiX spike control was used. Clusters were generated with a cluster generation kit (Illumina), cDNAs were sequenced by synthesis. Image analysis and base calling were realized with the HiSeq Control Software (Illumina) and the RTA software (Illumina), respectively. After a demultiplexing step, the sequences quality and the absence of contaminant were verified with the FastQC software and the FastQ Screen software, respectively. Raw data were submitted to a Purity Filter (Illumina) to remove overlapping clusters.

Alignment and counting

For each sample, the reads were pseudoaligned on the *S. frugiperda* reference transcriptome version OGS2.2 (25) using Bowtie2.2.3 (76). Processing of alignment files (.sam files) into sorted .bam files was performed by samtools view and samtools sort commands (77). Read counts for each gene were obtained using samtools idxstats command.

Differential expression analysis

Differential expression was analyzed with the R package DESeq2 (26). Treated versus untreated samples of the same tissue + time conditions were analyzed using a classical method. An example is shown in **S2 Data** for the analysis of differential expression in the fat body at 8 hpi identifying 5 DE genes at a p-value adjusted of 0.01, equivalent to 1% false discovery rate (**S2 Fig**).

For the global analysis of the EPN effect, we used the Likelihood Ratio test function of DESeq2 as presented in **S3 Data.** At an adjusted p-value of 0.1, this method identified 271 DE genes associated to EPN treatment. We overlapped this list with the pair-wise comparisons above to define tissue-specific or common responses as shown in **Fig 1E**.

Each sub list of DE genes has been analyzed with Blast2GO Pro software (78) to identify homolog sequences by blastx as well as GO categories. By using the full list of *S. frugiperda* OGS2.2 transcripts as reference (25), the enriched GO terms were identified with a Fisher's exact test (one-tailed, FDR < 0.05).

Heatmaps were generated using the heatmap.2 function of the gplots R package such as this presented in **S4 Data** that generated **Fig 1D**.

qPCR and primers

Differential expression data were verified with control RT-qPCR on selected upregulated and downregulated genes on independently performed EPN infestation experiments. cDNA was synthesized with SuperScript II Reverse Transcriptase (Invitrogen) from 1 µg of RNA sample, according to the manufacturer's protocol.

The primers (**S1 Table**) were designed with the Primer3Web tool (79). Their efficiency was estimated by using serial dilutions of pooled cDNA samples and their specificity was verified with melting curves analysis. Amplification and melting curves were analyzed with the LightCycler 480 software (Roche Molecular diagnostics) version 1.5.0.

RT-qPCR were carried out in triplicate for each biological sample, with the LightCycler 480 SYBR Green I Master kit (Roche Molecular diagnostics). For each couple of sample and primer, 1.25 µL of sample containing 50 ng/µL of cDNA and 1.75 µL of Master mix containing 0.85 µM of primers were distributed in multiwell plates by the Echo 525 liquid handler (Labcyte). After an enzyme activation step of 95°C for 15 min, the amplification was monitored in the LightCycler 480 (Roche) thermal cycler for 45 cycles of 95°C for 5 s, 60°C for 10 s and 72°C for 15 s.

Crossing points were determined using the Second Derivative Maximum method with the LightCycler 480 software (Roche Molecular diagnostics) version 1.5.0. Relative expression quantifications were then processed with the REST 2009 software (80), using the pairwise fixed randomization test with 2,000 permutations. Targets relative levels were normalized to RpL32 housekeeping gene relative levels and the EF1 gene was used as an internal control.

496 ## Acknowledgments

497 We thank the quarantine insect platform (PIQ), member of the Vectopole Sud network, for
498 providing the infrastructure needed for pest insect experimentations. We are also grateful to
499 Clotilde Gibard and Gaëtan Clabots for maintaining the insect collections of the DGIMI
500 laboratory in Montpellier.

501

References

1. Lacey LA, Grzywacz D, Shapiro-Ilan DI, Frutos R, Brownbridge M, Goettel MS. Insect pathogens as biological control agents: Back to the future. Journal of invertebrate pathology. 2015;132:1-41.
2. Ehlers RU, Hokkanen HMT. Insect biocontrol with non-endemic entomopathogenic nematodes (*Steinernema* and *Heterorhabditis* spp): Conclusions and recommendations of a combined OECD and COST Workshop on Scientific and Regulatory Policy Issues. Biocontrol Sci Techn. 1996;6(3):295-302.
3. Negrisoli AS, Garcia MS, Negrisoli CRCB, Bernardi D, da Silva A. Efficacy of entomopathogenic nematodes (Nematoda: Rhabditida) and insecticide mixtures to control *Spodoptera frugiperda* (Smith, 1797) (Lepidoptera: Noctuidae) in corn crops. Crop Prot. 2010;29(7):677-83.
4. Viteri DM, Linares AM, Flores L. Use of the entomopathogenic nematode *Steinernema carpocapsae* in combination with low-toxicity insecticides to control fall armyworm (Lepidoptera: Noctuidae) Larvae. Florida Entomologist. 2018;101(2):327-9.
5. Koppenhofer AM, Grewal PS, Fuzy EM. Differences in penetration routes and establishment rates of four entomopathogenic nematode species into four white grub species. Journal of invertebrate pathology. 2007;94(3):184-95.
6. Sicard M, Brugirard-Ricaud K, Pages S, Lanois A, Boemare NE, Brehelin M, et al. Stages of infection during the tripartite interaction between *Xenorhabdus nematophila*, its nematode vector, and insect hosts. Applied and environmental microbiology. 2004;70(11):6473-80.
7. Dowds BCA, Peters A. Virulence mechanisms. In: Gaugler R, editor. Entomopthogenic Nematology: CABI Publishing; 2002. p. 69-96.
8. Lemaitre B, Hoffmann JA. The host defense of *Drosophila melanogaster*. Annual Review of Immunology. 2007;25(1):697-743.
9. Tanaka H, Ishibashi J, Fujita K, Nakajima Y, Sagisaka A, Tomimoto K, et al. A genome-wide analysis of genes and gene families involved in innate immunity of *Bombyx mori*. Insect biochemistry and molecular biology. 2008;38(12):1087-110.
10. Zou Z, Evans JD, Lu ZQ, Zhao PC, Williams M, Sumathipala N, et al. Comparative genomic analysis of the *Tribolium* immune system. Genome Biol. 2007;8(8).
11. Cao X, He Y, Hu Y, Wang Y, Chen Y-R, Bryant B, et al. The immune signaling pathways of *Manduca sexta*. Insect biochemistry and molecular biology. 2015;62:64-74.
12. Evans JD, Aronstein K, Chen YP, Hetru C, Imler JL, Jiang H, et al. Immune pathways and defence mechanisms in honey bees *Apis mellifera*. Insect molecular biology. 2006;15(5):645-56.
13. Gerardo NM, Altincicek B, Anselme C, Atamian H, Barribeau SM, de Vos M, et al. Immunity and other defenses in pea aphids, *Acyrthosiphon pisum*. Genome Biol. 2010;11(2):R21.
14. Ferrandon D. The complementary facets of epithelial host defenses in the genetic model organism *Drosophila melanogaster*: from resistance to resilience. Current opinion in immunology. 2013;25(1):59-70.
15. Kristensen N, Chauvin G. Vol. IV: Lepidoptera, moths and butterflies. Morphology, physiology and development. Integument. In: Handbook of Zoology, W. de Gruyter Editor. 2012;2:1-8.
16. Lehane MJ. Peritrophic matrix structure and function. Annu Rev Entomol. 1997;42:525-50.
17. Strand MR. The insect cellular immune response. Insect Science. 2008;15(1):1-14.
18. Jiravanichpaisal P, Lee BL, Soderhall K. Cell-mediated immunity in arthropods: hematopoiesis, coagulation, melanization and opsonization. Immunobiology. 2006;211(4):213-36.

19. Nakhleh J, El Moussawi L, Osta MA. Chapter Three - The Melanization Response in Insect Immunity. In: Ligoxygakis P, editor. Advances in Insect Physiology. 52: Academic Press; 2017. p. 83-109.
20. Ferrandon D, Imler JL, Hetru C, Hoffmann JA. The *Drosophila* systemic immune response: sensing and signalling during bacterial and fungal infections. Nature reviews immunology. 2007;7(11):862-74.
21. Issa N, Guillaumot N, Lauret E, Matt N, Schaeffer-Reiss C, Van Dorsselaer A, et al. The circulating protease Persephone is an immune sensor for microbial proteolytic activities upstream of the *Drosophila* Toll pathway. Mol Cell. 2018;69(4):539-50 e6.
22. Arefin B, Kucerova L, Dobes P, Markus R, Strnad H, Wang Z, et al. Genome-wide transcriptional analysis of *Drosophila* larvae infected by entomopathogenic nematodes shows involvement of complement, recognition and extracellular matrix proteins. J Innate Immun. 2014;6(2):192-204.
23. Castillo JC, Creasy T, Kumari P, Shetty A, Shokal U, Tallon LJ, et al. *Drosophila* anti-nematode and antibacterial immune regulators revealed by RNA-Seq. BMC genomics. 2015;16:519.
24. Yadav S, Daugherty S, Shetty AC, Eleftherianos I. RNAseq analysis of the *Drosophila* response to the entomopathogenic nematode *Steinernema*. G3 (Bethesda). 2017;7(6):1955-67.
25. Gouin A, Bretaudeau A, Nam K, Gimenez S, Aury JM, Duvic B, et al. Two genomes of highly polyphagous lepidopteran pests (*Spodoptera frugiperda*, Noctuidae) with different host-plant ranges. Scientific reports. 2017;7(1):11816.
26. Love MI, Huber W, Anders S. Moderated estimation of fold change and dispersion for RNA-seq data with DESeq2. Genome Biol. 2014;15(12):550.
27. Zhang L, Wang YW, Lu ZQ. Midgut immune responses induced by bacterial infection in the silkworm, *Bombyx mori*. Journal of Zhejiang University Science B. 2015;16(10):875-82.
28. Biteau B, Karpac J, Supoyo S, Degennaro M, Lehmann R, Jasper H. Lifespan extension by preserving proliferative homeostasis in *Drosophila*. PLoS Genet. 2010;6(10):e1001159.
29. Feyereisen R. Insect P450 enzymes. Annu Rev Entomol. 1999;44:507-33.
30. Kleino A, Valanne S, Ulvila J, Kallio J, Myllymaki H, Enwald H, et al. Inhibitor of apoptosis 2 and TAK1-binding protein are components of the Drosophila Imd pathway. The EMBO journal. 2005;24(19):3423-34.
31. Arrese EL, Soulages JL. Insect fat body: energy, metabolism, and regulation. Annu Rev Entomol. 2010;55:207-25.
32. Lemaitre B, Nicolas E, Michaut L, Reichhart JM, Hoffmann JA. The dorsoventral regulatory gene cassette spatzle/Toll/cactus controls the potent antifungal response in *Drosophila* adults. Cell. 1996;86(6):973-83.
33. Weber AN, Tauszig-Delamasure S, Hoffmann JA, Lelievre E, Gascan H, Ray KP, et al. Binding of the *Drosophila* cytokine Spatzle to Toll is direct and establishes signaling. Nature immunology. 2003;4(8):794-800.
34. Lavine MD, Strand MR. Insect hemocytes and their role in immunity. Insect biochemistry and molecular biology. 2002;32(10):1295-309.
35. Bidla G, Lindgren M, Theopold U, Dushay MS. Hemolymph coagulation and phenoloxidase in Drosophila larvae. Developmental and Comparative Immunology. 2005;29(8):669-79.
36. Kanost MR, Gorman MJ. Phenoloxidases in insect immunity. In: Beckage NE, editor. Insect Immunology. San Diego: Academic Press; 2008. p. 69-96.
37. Lu A, Zhang Q, Zhang J, Yang B, Wu K, Xie W, et al. Insect prophenoloxidase: the view beyond immunity. Frontiers in physiology. 2014;5:252-.
38. Bartholomay LC, Cho WL, Rocheleau TA, Boyle JP, Beck ET, Fuchs JF, et al. Description of the transcriptomes of immune response-activated hemocytes from the mosquito vectors Aedes aegypti and Armigeres subalbatus. Infect Immun. 2004;72(7):4114-26.

608 39. Dimopoulos G, Christophides GK, Meister S, Schultz J, White KP, Barillas-Mury C, et
609 al. Genome expression analysis of Anopheles gambiae: responses to injury, bacterial
610 challenge, and malaria infection. Proceedings of the National Academy of Sciences of the
611 United States of America. 2002;99(13):8814-9.
612 40. Irving P, Ubeda JM, Doucet D, Troxler L, Lagueux M, Zachary D, et al. New insights
613 into Drosophila larval haemocyte functions through genome-wide analysis. Cell Microbiol.
614 2005;7(3):335-50.
615 41. Jiang H, Wang Y, Gu Y, Guo X, Zou Z, Scholz F, et al. Molecular identification of a
616 bevy of serine proteinases in *Manduca sexta* hemolymph. Insect biochemistry and molecular
617 biology. 2005;35(8):931-43.
618 42. Kanost MR, Jiang H. Clip-domain serine proteases as immune factors in insect
619 hemolymph. Curr Opin Insect Sci. 2015;11:47-55.
620 43. Haghayeghi A, Sarac A, Czerniecki S, Grosshans J, Schock F. Pellino enhances
621 innate immunity in *Drosophila*. Mech Dev. 2010;127(5-6):301-7.
622 44. Ji S, Sun M, Zheng X, Li L, Sun L, Chen D, et al. Cell-surface localization of Pellino
623 antagonizes Toll-mediated innate immune signalling by controlling MyD88 turnover in
624 *Drosophila*. Nat Commun. 2014;5:3458.
625 45. Volkoff AN, Rocher J, d'Alencon E, Bouton M, Landais I, Quesada-Moraga E, et al.
626 Characterization and transcriptional profiles of three Spodoptera frugiperda genes encoding
627 cysteine-rich peptides. A new class of defensin-like genes from lepidopteran insects? Gene.
628 2003;319:43-53.
629 46. Destoumieux-Garzon D, Brehelin M, Bulet P, Boublik Y, Girard PA, Baghdiguian S, et
630 al. Spodoptera frugiperda X-tox protein, an immune related defensin rosary, has lost the
631 function of ancestral defensins. PloS one. 2009;4(8):e6795.
632 47. Michel T, Reichhart JM, Hoffmann JA, Royet J. *Drosophila* Toll is activated by Gram-
633 positive bacteria through a circulating peptidoglycan recognition protein. Nature.
634 2001;414(6865):756-9.
635 48. Zhao S, Wang X, Cai S, Zhang S, Luo H, Wu C, et al. A novel peptidoglycan
636 recognition protein involved in the prophenoloxidase activation system and antimicrobial
637 peptide production in *Antheraea pernyi*. Dev Comp Immunol. 2018;86:78-85.
638 49. Krautz R, Arefin B, Theopold U. Damage signals in the insect immune response.
639 Front Plant Sci. 2014;5(342).
640 50. Qiao C, Li J, Wei XH, Wang JL, Wang YF, Liu XS. SRP gene is required for
641 *Helicoverpa armigera* prophenoloxidase activation and nodulation response. Dev Comp
642 Immunol. 2014;44(1):94-9.
643 51. Senger K, Harris K, Levine M. GATA factors participate in tissue-specific immune
644 responses in *Drosophila* larvae. Proceedings of the National Academy of Sciences of the
645 United States of America. 2006;103(43):15957-62.
646 52. Vilcinskas A, Wedde M. Insect inhibitors of metalloproteinases. IUBMB life.
647 2002;54(6):339-43.
648 53. Wedde M, Weise C, Kopacek P, Franke P, Vilcinskas A. Purification and
649 characterization of an inducible metalloprotease inhibitor from the hemolymph of greater wax
650 moth larvae, *Galleria mellonella*. European journal of biochemistry. 1998;255(3):535-43.
651 54. Clermont A, Wedde M, Seitz V, Podsiadlowski L, Lenze D, Hummel M, et al. Cloning
652 and expression of an inhibitor of microbial metalloproteinases from insects contributing to
653 innate immunity. Biochem J. 2004;382(Pt 1):315-22.
654 55. Schmidt TM, Bleakley B, Nealson KH. Characterization of an extracellular protease
655 from the insect pathogen *Xenorhabdus luminescens*. Applied and environmental
656 microbiology. 1988;54(11):2793-7.
657 56. Caldas C, Cherqui A, Pereira A, Simões N. Purification and characterization of an
658 extracellular protease from *Xenorhabdus nematophila* involved in insect
659 immunosuppression. Applied and environmental microbiology. 2002;68(3):1297-304.
660 57. Massaoud MK, Marokhazi J, Venekei I. Enzymatic characterization of a serralysin-
661 like metalloprotease from the entomopathogen bacterium, *Xenorhabdus*. Biochimica et
662 biophysica acta. 2011;1814(10):1333-9.

58. Ishii K, Adachi T, Hara T, Hamamoto H, Sekimizu K. Identification of a *Serratia marcescens* virulence factor that promotes hemolymph bleeding in the silkworm, *Bombyx mori*. Journal of invertebrate pathology. 2014;117:61-7.
59. Peng D, Lin J, Huang Q, Zheng W, Liu G, Zheng J, et al. A novel metalloproteinase virulence factor is involved in *Bacillus thuringiensis* pathogenesis in nematodes and insects. Environmental microbiology. 2016;18(3):846-62.
60. Myllymaki H, Valanne S, Ramet M. The *Drosophila* imd signaling pathway. Journal of immunology. 2014;192(8):3455-62.
61. Kakumani PK, Malhotra P, Mukherjee SK, Bhatnagar RK. A draft genome assembly of the army worm, *Spodoptera frugiperda*. Genomics. 2014;104(2):134-43.
62. Nandakumar S, Ma H, Khan AS. Whole-genome sequence of the *Spodoptera frugiperda* Sf9 insect cell line. Genome announcements. 2017;5(34).
63. Cheng T, Wu J, Wu Y, Chilukuri RV, Huang L, Yamamoto K, et al. Genomic adaptation to polyphagy and insecticides in a major East Asian noctuid pest. Nature ecology & evolution. 2017;1(11):1747-56.
64. Pearce SL, Clarke DF, East PD, Elfekih S, Gordon KHJ, Jermiin LS, et al. Genomic innovations, transcriptional plasticity and gene loss underlying the evolution and divergence of two highly polyphagous and invasive *Helicoverpa* pest species. BMC biology. 2017;15(1):63.
65. Minakhina S, Yang J, Steward R. Tamo selectively modulates nuclear import in Drosophila. Genes to Cells. 2003;8(4):299-310.
66. Chou S, Daugherty MD, Peterson SB, Biboy J, Yang Y, Jutras BL, et al. Transferred interbacterial antagonism genes augment eukaryotic innate immune function. Nature. 2015;518(7537):98-101.
67. Aymeric JL, Givaudan A, Duvic B. Imd pathway is involved in the interaction of *Drosophila melanogaster* with the entomopathogenic bacteria, *Xenorhabdus nematophila* and *Photorhabdus luminescens*. Mol Immunol. 2010;47(14):2342-8.
68. Mastore M, Arizza V, Manachini B, Brivio MF. Modulation of immune responses of *Rhynchophorus ferrugineus* (Insecta: Coleoptera) induced by the entomopathogenic nematode *Steinernema carpocapsae* (Nematoda: Rhabditida). Insect Sci. 2015;22(6):748-60.
69. Ji D, Kim Y. An entomopathogenic bacterium, Xenorhabdus nematophila, inhibits the expression of an antibacterial peptide, cecropin, of the beet armyworm, Spodoptera exigua. Journal of insect physiology. 2004;50(6):489-96.
70. Pena JM, Carrillo MA, Hallem EA. Variation in the susceptibility of *Drosophila* to different entomopathogenic nematodes. Infect Immun. 2015;83(3):1130-8.
71. Binda-Rossetti S, Mastore M, Protasoni M, Brivio MF. Effects of an entomopathogen nematode on the immune response of the insect pest red palm weevil: Focus on the host antimicrobial response. Journal of invertebrate pathology. 2016;133:110-9.
72. Duvic B, Jouan V, Essa N, Girard PA, Pages S, Khattar ZA, et al. Cecropins as a marker of *Spodoptera frugiperda* immunosuppression during entomopathogenic bacterial challenge. Journal of insect physiology. 2012;58(6):881-8.
73. Poitout S. Elevage de plusieurs espèces de Lépidoptères Noctuidae sur milieu artificiel riche et sur milieu artificiel simplifié. Ann Zool Ecol Anim. 1970;2:79-91.
74. White GF. A method for obtaining infective nematode larvae from cultures. Science. 1927;66(1709):302-3.
75. van Sambeek J, Wiesner A. Successful parasitation of locusts by entomopathogenic nematodes is correlated with inhibition of insect phagocytes. Journal of invertebrate pathology. 1999;73(2):154-61.
76. Langmead B, Salzberg SL. Fast gapped-read alignment with Bowtie 2. Nature methods. 2012;9(4):357-9.
77. Li H, Handsaker B, Wysoker A, Fennell T, Ruan J, Homer N, et al. The sequence alignment/map format and SAMtools. Bioinformatics (Oxford, England). 2009;25(16):2078-9.

78. Conesa A, Gotz S, Garcia-Gomez JM, Terol J, Talon M, Robles M. Blast2GO: a universal tool for annotation, visualization and analysis in functional genomics research. Bioinformatics (Oxford, England). 2005;21(18):3674-6.
79. Untergasser A, Cutcutache I, Koressaar T, Ye J, Faircloth BC, Remm M, et al. Primer3 - New capabilities and interfaces. Nucleic acids research. 2012;40(15):e115.
80. Pfaffl MW, Horgan GW, Dempfle L. Relative expression software tool (REST) for group-wise comparison and statistical analysis of relative expression results in real-time PCR. Nucleic acids research. 2002;30(9):e36.
81. Le SQ, Gascuel O. An improved general amino acid replacement matrix. Mol Biol Evol. 2008;25(7):1307-20.
82. Felsenstein J. Confidence limits on phylogenies: An approach using the bootstrap. Evolution; international journal of organic evolution. 1985;39(4):783-91.

729 # Figure Legends

730 **Fig 1: Tissue specific transcriptional response time series of *Spodoptera frugiperda***
731 **larvae to EPN infestation**

732 **A:** Overview of the experimental design. In three independent experiments, 9 infested and 9
733 control larvae from culture plates were dissected at 8 hpi and 15 hpi. Hemocytes, fat bodies
734 and midguts were extracted and pooled by organ for each time and condition. Polyadenylated
735 RNAs were purified from these pools and corresponding cDNA libraries were built. cDNAs
736 were sequenced on a single end by Illumina and RNAseq data were analyzed to identify the
737 genes that are differentially expressed during *Steinernema carpocapsae* infestation.
738 **B:** Growth of *Xenorhabdus nematophila* following *S. frugiperda* infestation with 150
739 symbiotic *S. carpocapsae*. At 8 hpi and 15 hpi, the number of CFU per mL of hemolymph was
740 estimated from three independent experiments with three technical replicates (three larvae per
741 technical replicate). Error bars indicate standard errors of the means.
742 **C:** Survival curve. Larvae were infested with 150 nematobacterial IJ. Data represent means
743 ± SEs of four independent experiments, each containing 12 larvae.
744 **D:** EPN effect significant gene response. This heatmap shows z-score of expression variation
745 across all RNAseq samples (red being overexpressed and blue under-expressed) for 271 genes
746 with significant variations to EPN infestation.
747 **E:** Venn diagram showing the tissue specificity of the EPN responsive genes at 15 hpi. The
748 response can be overexpression (Up:U) or under-expression (Down:D). For example, there are
749 71 genes varying significantly upon EPN infestation in both the fat body (FB) and the
750 hemocytes (HC). Of these, 66 are up-regulated in both tissues (UU), 3 are down-regulated in
751 both tissues (DD) and 2 are down-regulated in FB and up-regulated in HC (DU). By
752 convention, the order of the U and D letters represent respectively MG, FB and HC tissues.
753

Fig 2: Midgut Associated Response

Heatmaps of differential expression (in log2FoldChange - green, under-expression, red, overexpression according to values in **S1 Data**) across all experimental conditions of genes found significantly differentially expressed **A**: specifically in the MG at 15 hpi (MG15 - 4 genes) **B**: common to MG15 and FB15 (9 genes) and **C**: common to MG15 and HC15 (10 genes).

Fig 3: Fat body and hemocytes associated responses

As in **Fig 2**, heatmaps of differential expression for genes **A:** specific to FB15 (14 genes), **B:** specific to HC15 (77 genes) and **C**: common to FB15 and HC15 (71 genes).

Fig 4: IMPI

A: WebApollo viewer showing the annotation of inducible metalloprotease inhibitors genes in cluster on the scaffold_1741 in the genome of *Spodoptera frugiperda*. **B:** As in **Fig 2**, heatmap of differential expression for the identified IMPI genes.

Fig 5: Common tissues

A: As in **Fig 2 and 3**, heatmap of differential expression for the 31 genes common to MG15, FB15 and HC15. **B:** WebApollo viewer showing the annotation of unknown genes in cluster on the scaffold_520. **C:** WebApollo viewer showing the annotation of clustered genes of bacterial origin within a defensin cluster.

S1 Table: Primers sequences and genes

S1 Data: Differentially Expressed (DE) genes at 15 hpi

This table presents the genes that are found differentially expressed upon EPN infestation at 15 hpi. The baseMean column represents the DESeq2 normalized mean expression levels of a particular gene across all experiments. The log2FoldChange and padj columns provided are given by the DESeq2 'results' command from pair-wise comparisons between (Midgut: MG, Fat Body: FB, Hemocytes: HC). On the right hand of the table, we present the best blastp homolog of each gene as well as our manual annotation of each gene based on this homology and protein domain analyses or on previous annotation (25)(in bold). Genes have been grouped by tissues where the differential expression false discovery rate (padj) was less than 0.01.

S2 Data: Script used for the analysis of differential expression in the fat body at 8 hpi.

S3 Data: Script for global analysis of the EPN effect.

S4 Data: Heatmaps were generated using the heatmap.2 function of the gplots R package such as below that generated Fig 1D.

S1 Fig: Dataset quality control

A: Heatmap of pair-wise correlation between all RNAseq samples. Hierarchical clustering of samples shows the grouping of experiments mostly by tissues then by time-point and by condition. **B:** Principal Component analysis of RNAseq samples showing the grouping of experiments mostly by tissue then by time-point and by condition.

S2 Fig: DESeq2 analysis

MA plots showing the log2FoldChange in function of mean expression (measured in reads coverage) of total *S. frugiperda* transcripts in a pairwise DESeq2 analysis of EPN vs PBS in

804 every Tissue*Time-point conditions. Indicated on each plot is the number of genes
805 significantly overexpressed (red box) or under-expressed (blue box) upon EPN infestation. For
806 experiments at 15 hpi, the total number of DE genes is also indicated on the right side of the
807 plot.
808
809 **S3 Fig: DE genes in fat body at 8 hpi**
810 At 8 hpi, 5 genes are significantly differentially expressed in the fat body (FB08). This heatmap
811 of log2FoldChange shows that the 4 unknown genes significantly overexpressed in the FB08
812 condition are also overexpressed at 15 hpi in all 3 tissues. On the right hand side, this table
813 indicates the DESeq2 results for these genes, showing that the 4 overexpressed genes are of
814 unknown function and correspond to the gene cluster presented in **Fig 5B**.
815
816 **S4 Fig: Validation of RNAseq data using quantitative RT-PCR**
817 Selected genes were analyzed by quantitative PCR using RNA samples from tissues of naïve
818 or infected larvae. The relative expression level (ratio infected/naïve larvae) is shown as
819 log2FoldChange mean from 3 independent experiments.
820
821 **S5 Fig: Fat Body and Hemocytes Gene Ontology enrichment**
822 The DE genes common to FB and HC at 15 hpi (**Fig 3C**) show an enrichment of Gene Ontology
823 terms associated to immunity. The same analysis conducted on the other gene lists, in particular
824 the 77 genes associated to HC15, did not produce significant GO term enrichments.
825
826 **S6 Fig: Structures and phylogeny of *Spodoptera frugiperda* peptidoglycan recognition**
827 **proteins**

828 **A:** Structures of *Sf*PGRP. In red, signal peptide and in blue, transmembrane domain. **B:** The
829 phylogeny of 95 PGRP domain amino acid sequences was determined by using the Maximum
830 Likelihood method (81) in MEGA7 (82). The bootstrap consensus tree was built from 100
831 replicates and branches corresponding to partitions reproduced in less than 50% bootstrap
832 replicates were collapsed. Initial tree(s) for the heuristic search were obtained automatically by
833 applying Neighbor-Join and BioNJ algorithms to a matrix of pairwise distances estimated using
834 a JTT model, and then selecting the topology with superior log likelihood value. Branches
835 colors: green, Lepidopteran (Bm: *Bombyx mori*, Dp: *Danaus plexippus*, Hm: *Heliconius*
836 *melpomene*, Px: *Papillio xuthus*, Sf: *Spodoptera frugiperda*), bleu, Dipteran (Aa: *Aedes*
837 *aegypti*, Ag: *Anopheles gambiae*, Dm: *Drosophila melanogaster*) and orange, Hymenopteran
838 (Am: *Apis mellifera*, Nv: *Nasonia vitripennis*).
839
840 **S7 Fig: Phylogenetic analysis of genes from bacterial origin**
841 The 100 first best hits after blastp on nr NCBI were retrieved and the phylogenetic tree was
842 constructed using the method described as in **S6 Fig**. Sequences are grouped in two main
843 clades, one with bacteria only and the second with Lepidoptera only.

Fig 1

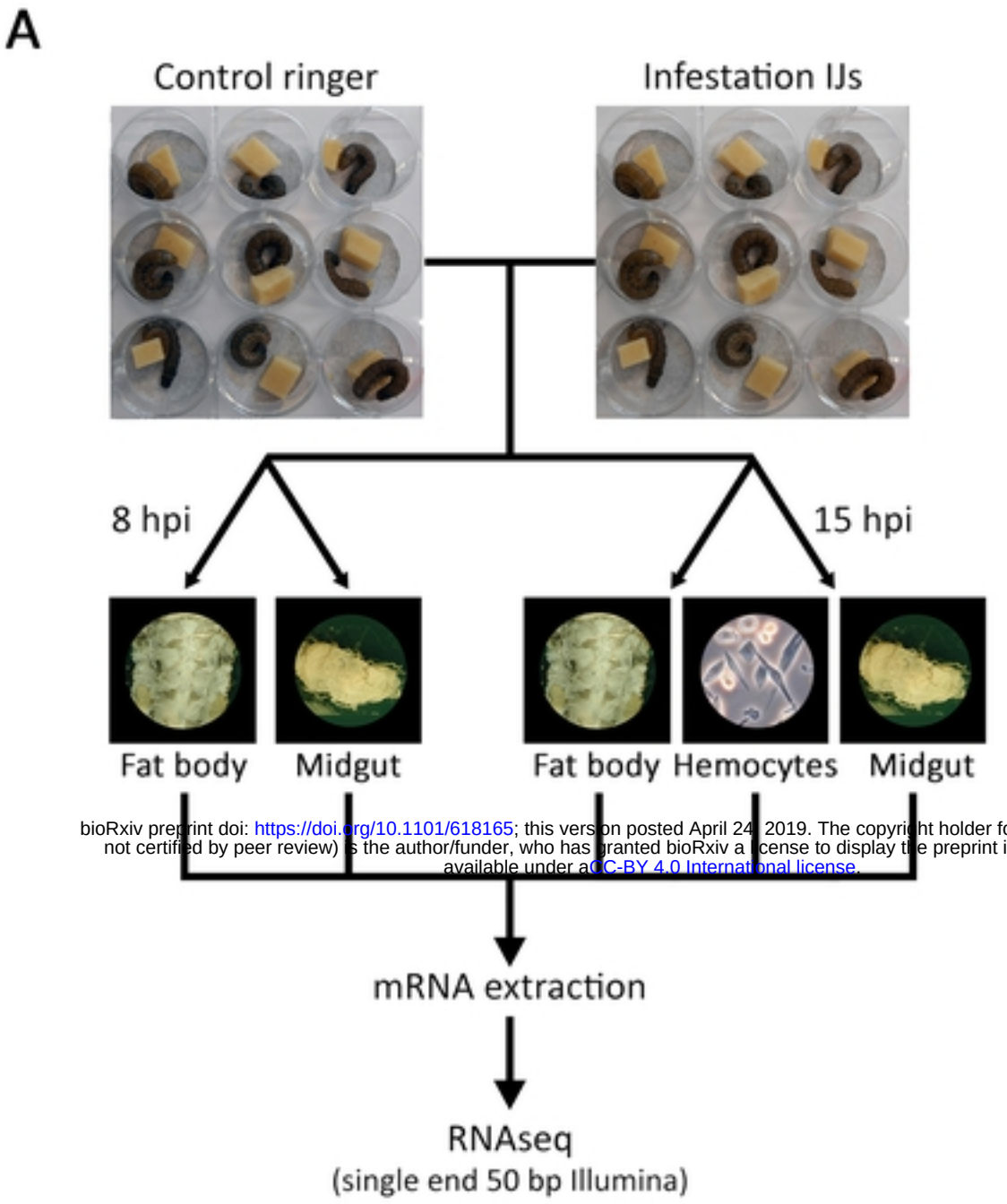

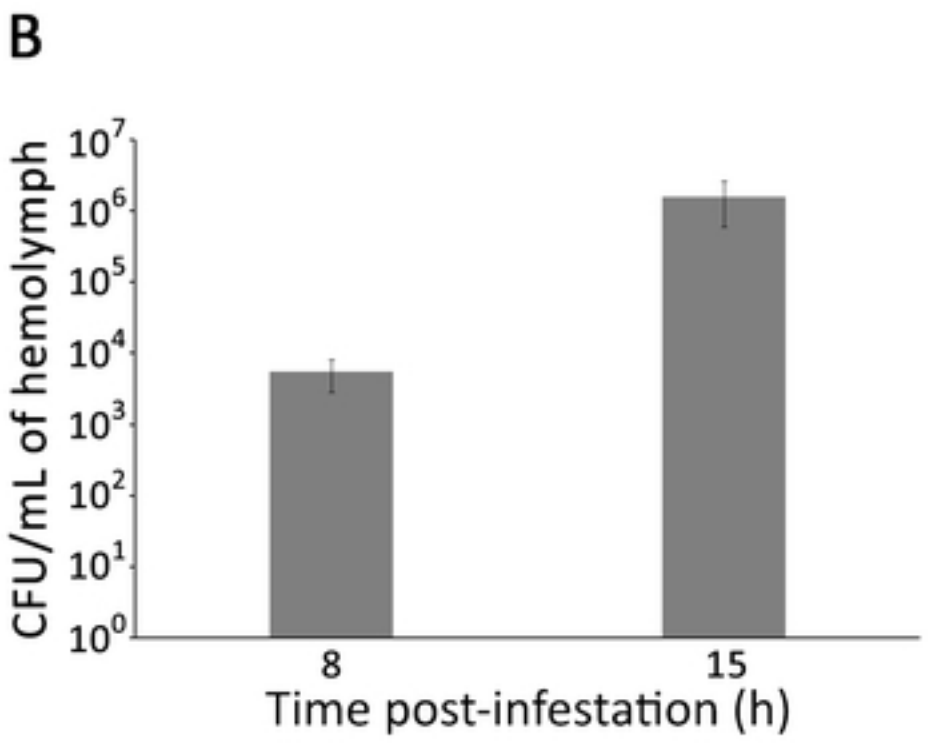

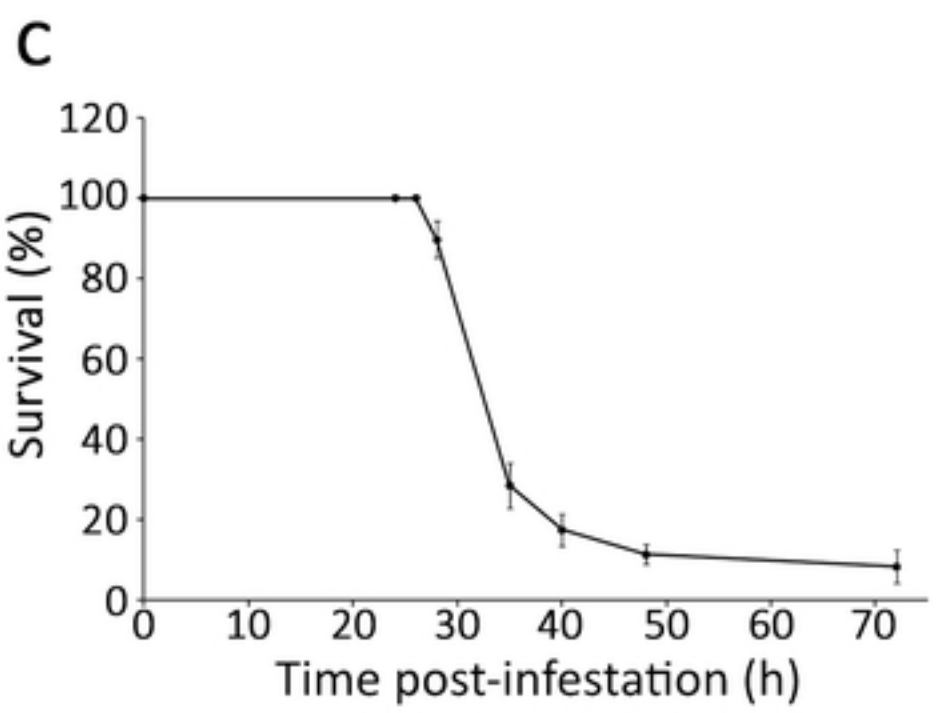

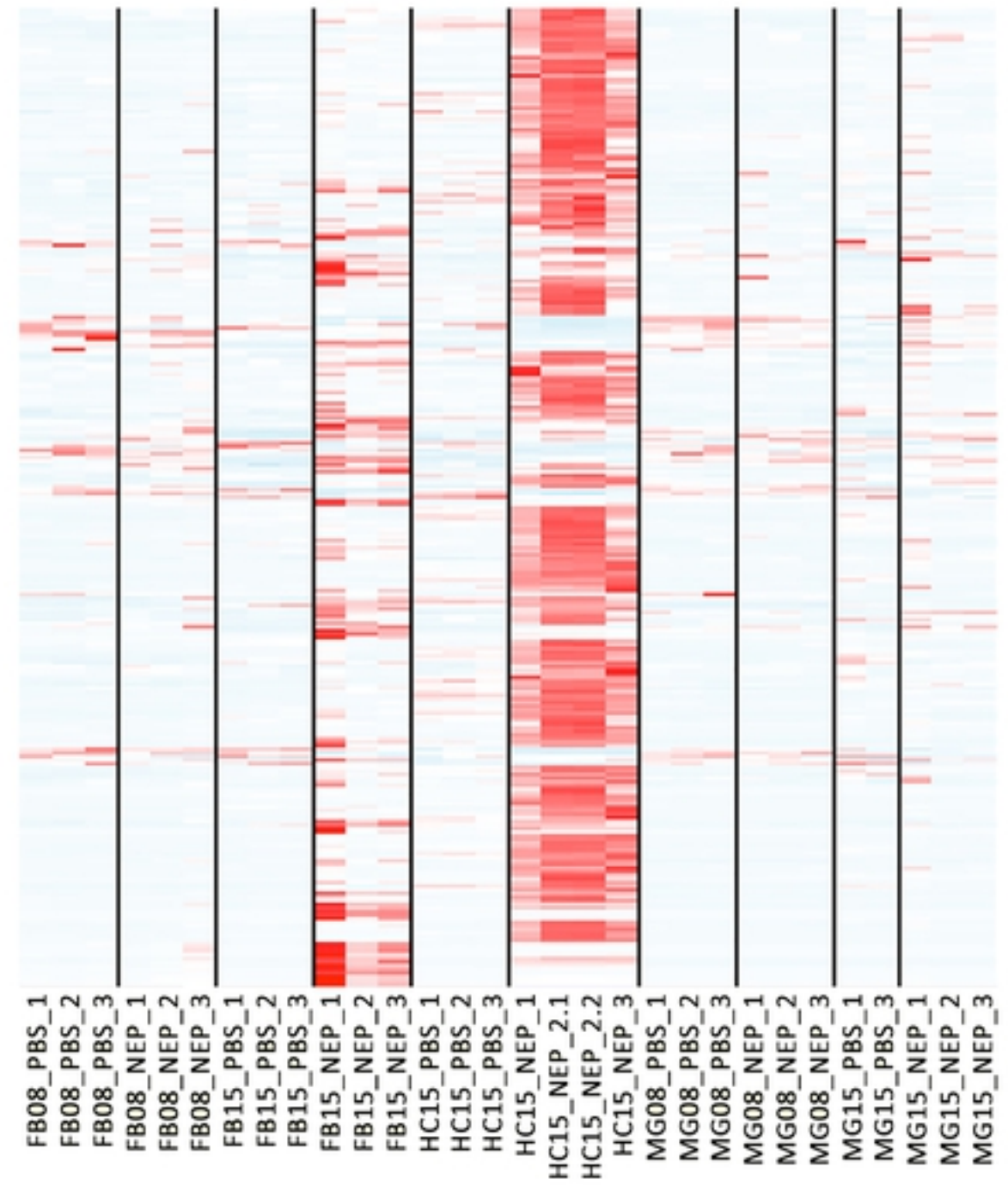

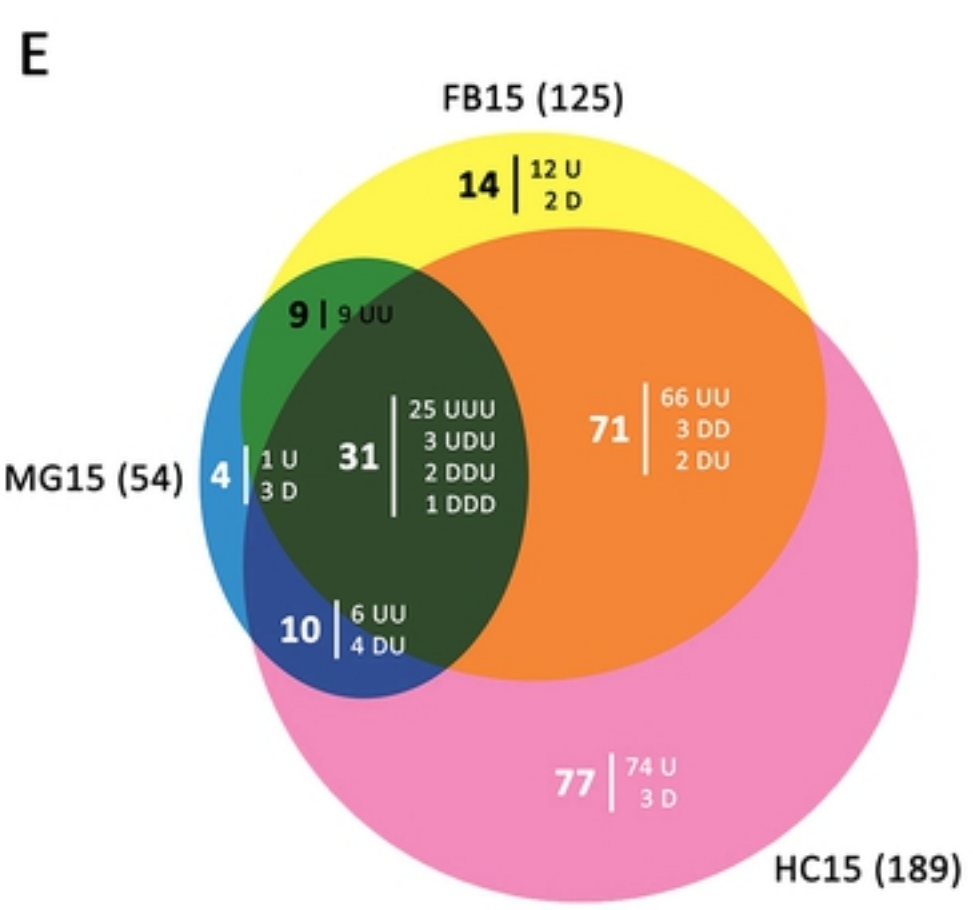

Figure 1

Fig 2

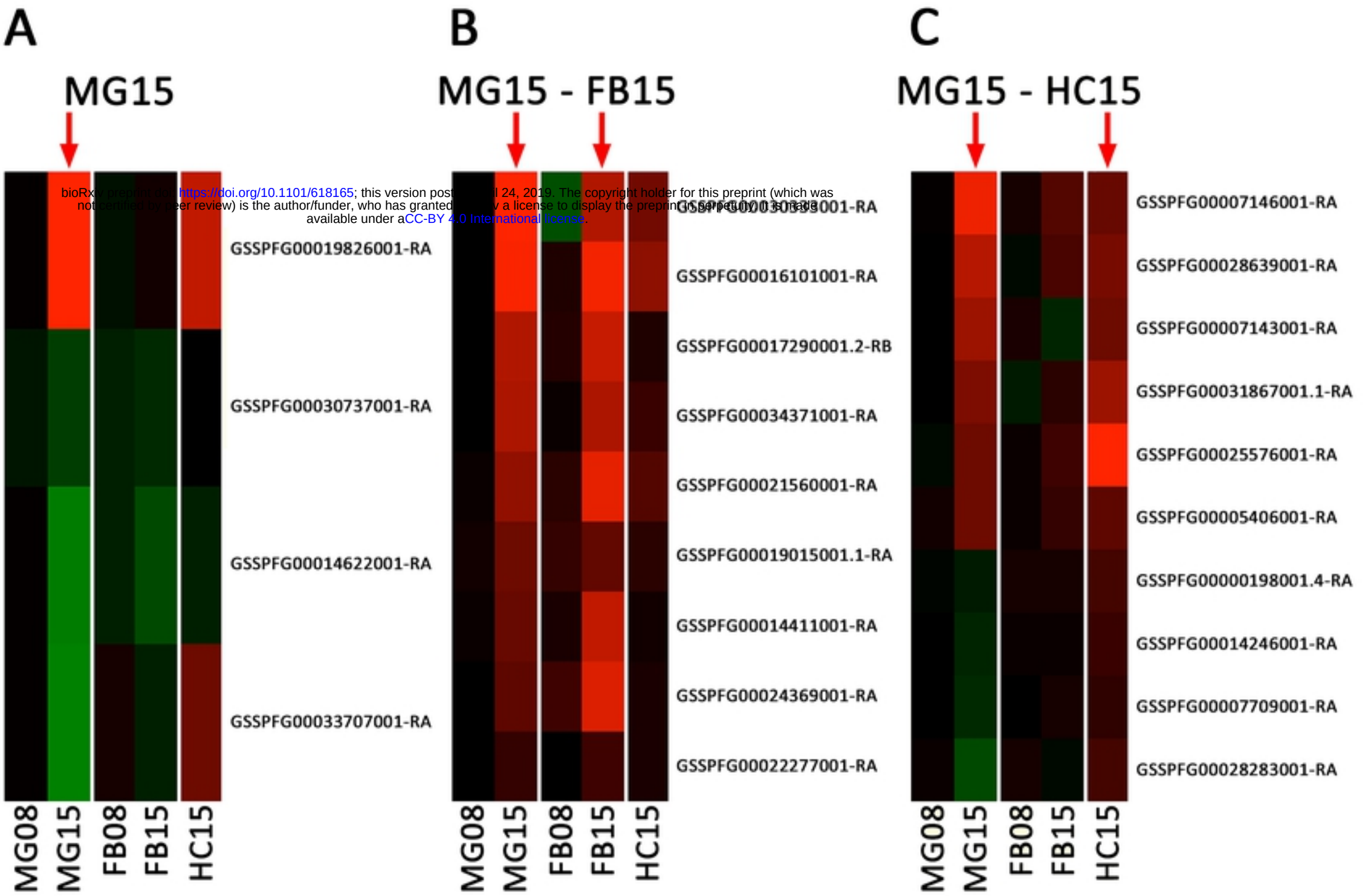

Figure 2

Fig 3

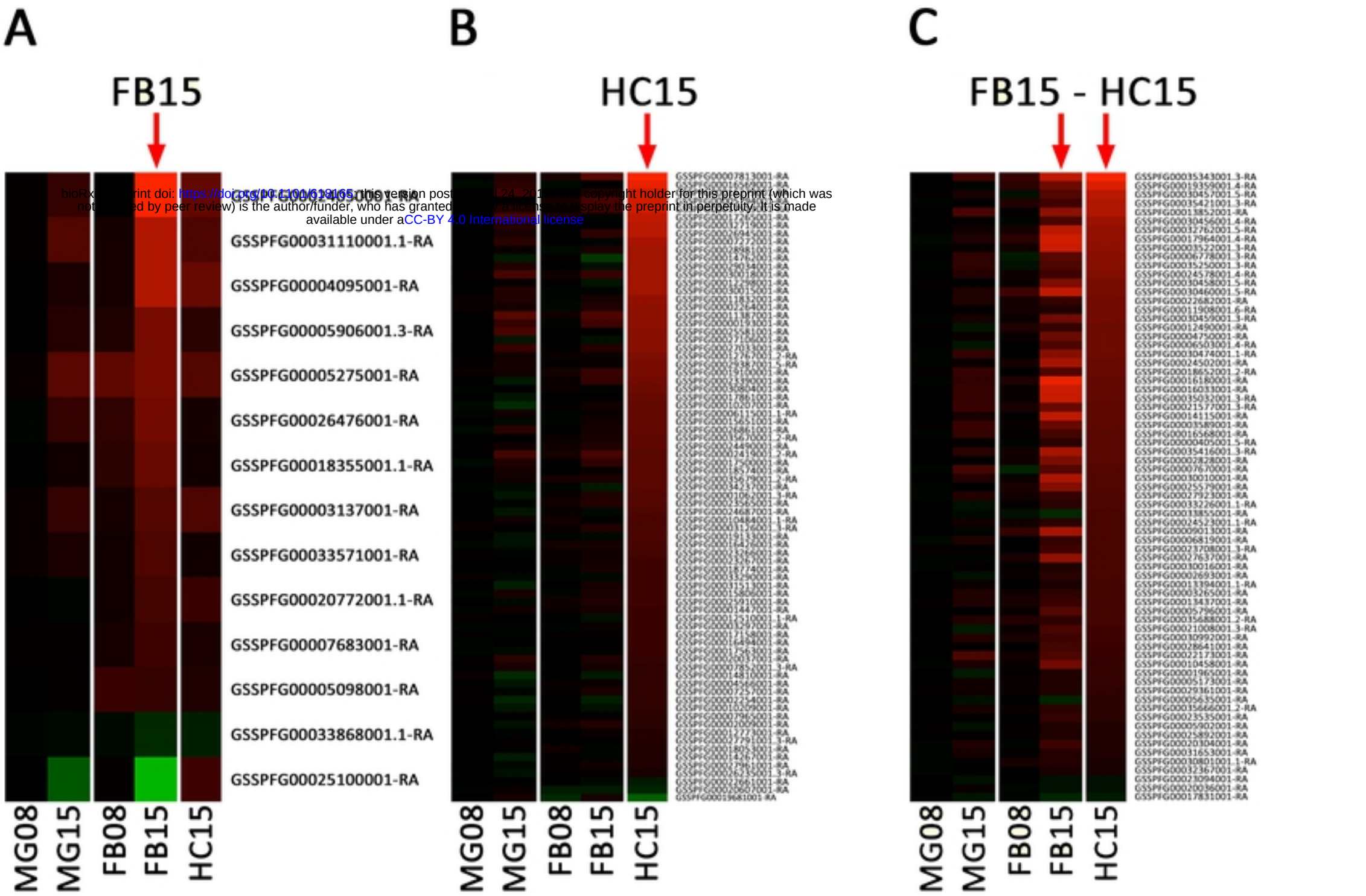

Figure 3

Fig 4

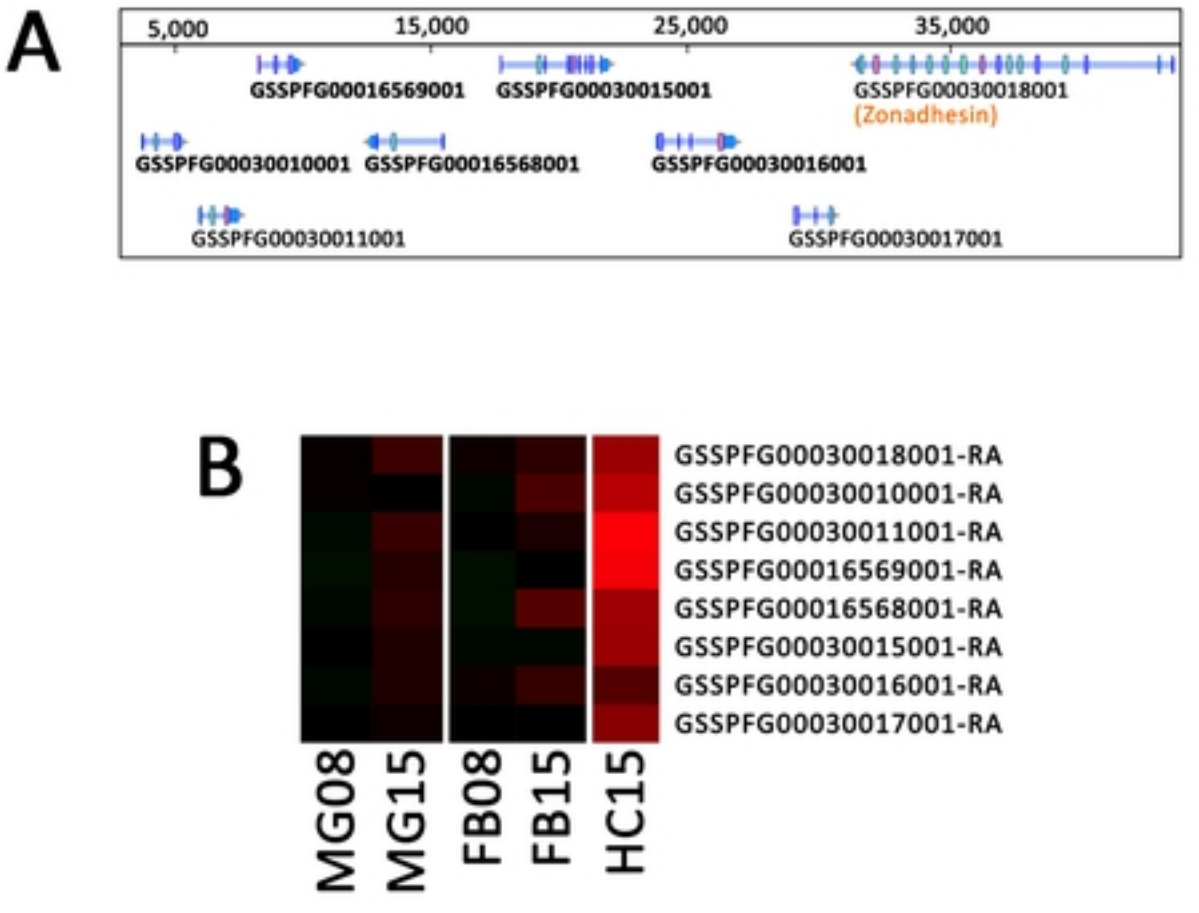

Figure 4

Fig 5

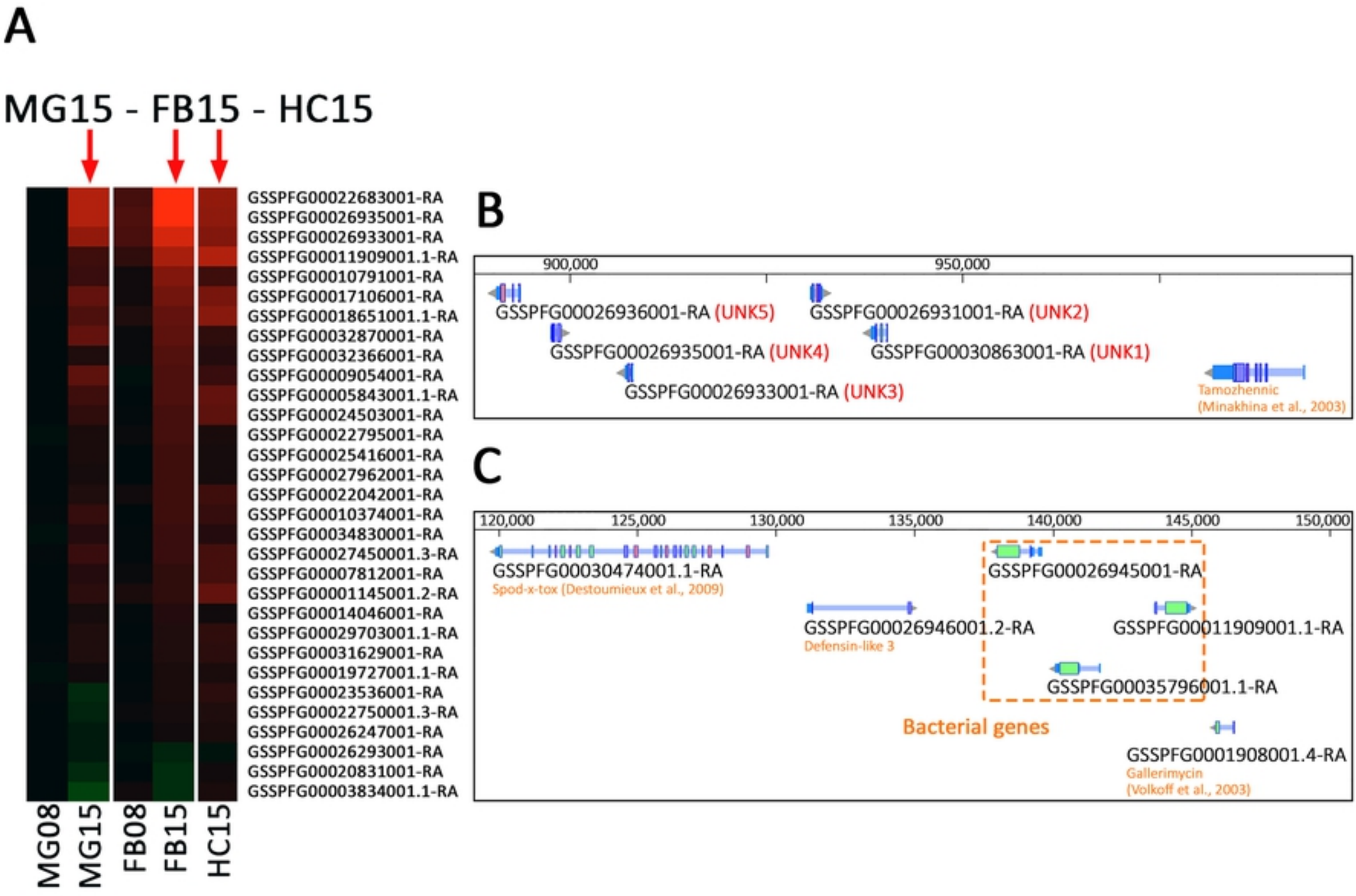

Figure 5